ARTICLE
Integrative Medicine Discovery 2025;9:e25005. https://doi.org/10.53388/IMD202509005

Chinese medicine *Bupleuri Radix* inhibits the proliferation of renal clear cell carcinoma is related to RORγ

Yan Li[1, 2, 3, 4#], Hao-Yu Wang[1, 2, 3, 4#], An-Qi Lv[1, 2, 3, 5], Xun Xu[1, 2, 3, 4], Wei Yan[1, 2, 3, 4], Lang Guo[1, 2, 3, 4], Zhong-Min Zhang[1, 2, 3, 4], Bing-Qi Zhang[1, 2, 3, 5*], Zheng-Ming Liao[1, 2, 3, 4*]

[1]The First Clinical College of Hubei University of Traditional Chinese Medicine, Wuhan 430065, China. [2]Department of Urology, Hubei Provincial Hospital of Traditional Chinese Medicine, Wuhan 430061, China. [3]Hubei Sizhen Laboratory, Wuhan 430061, China. [4]Affiliated Hospital of Hubei University of Chinese Medicine, Wuhan 430061, China. [5]College of Traditional Chinese Medicine, Hubei University of Traditional Chinese Medicine, Wuhan 430065, China.

[#]These authors contributed equally to this work and are co-first authors for this paper.
[*]**Correspondence to:** Bing-Qi Zhang, College of Traditional Chinese Medicine, Hubei University of Traditional Chinese Medicine, No. 16, Huangjiahu West Road, Wuhan 430065, China. E-mail: 18942947296@163.com. Zheng-Ming Liao, Department of Urology, Hubei Provincial Hospital of Traditional Chinese Medicine, No. 4, Garden Hill, Grain Road Street, Rouge Road, Wuchang District, Wuhan 430061, China. E-mail: lzmwhu@163.com.

Abstract

Background: This research aims to investigate potential gene targets and mechanisms through which the traditional Chinese medicine (TCM) *Bupleuri Radix* (Chaihu) may impact on clear cell renal cell carcinoma (ccRCC) treatment. **Methods:** Public databases were employed to identify Cedrenol, an active component of *Bupleuri Radix*, and its associated gene targets. Among these, the gene *RORC* (also known as *RORγ*) was selected for detailed analysis due to its high expression correlation. Expression levels of *RORC* across various cancers were assessed using the TCGA pan-cancer dataset. Further analyses, including differential expression, prognostic relevance, immune infiltration, single-gene, and functional enrichment analyses, were conducted using the TCGA ccRCC dataset. Additionally, potential drug sensitivities and molecular docking interactions with *RORC* were explored using the GSCALite and CellMiner databases. The effects of *RORC* on ccRCC were also validated through cellular experiments. **Results:** *RORC* exhibited elevated expression in clear cell renal carcinoma tissue in contrast to normal tissues, and lower *RORC* expression was related to better prognosis. Immune cell infiltration analysis suggested that *RORC* may influence the penetration of cells that inhibit immune responses, such as regulatory T cells, thereby affecting ccRCC progression. Furthermore, molecular docking studies revealed that several drugs, including Axitinib, Docetaxel, Methotrexate, and Temsirolimus, have a high affinity for *RORC* and exhibit strong molecular binding. In cellular experiment experiments confirmed that *RORC* knockdown led to reduced proliferation, metastasis, and ccRCC cell invasion. **Conclusion:** The study implies that *RORC* may be a potential gene target for *Bupleuri Radix* in the management of ccRCC.

Keywords: traditional Chinese medicine; *Bupleuri Radix* (Chaihu); clear cell renal cell carcinoma; urologic neoplasms; RORC (RORγ)

Author contributions

Li Y and Wang HY contributed equally to this work. Li Y, Lv AQ and Wang HY: Conceptualization, data analysis, validation, writing, molecular biology experiments, data analysis and editing the manuscript. Xu X and Zhang BQ: Collection of information. Guo L, Liao ZM, Yan W and Zhang ZM: investigation, review and editing. All authors read and approved the final manuscript.

Competing interests

The authors declare no conflicts of interest.

Acknowledgments

We thank TCMSP, GEO, TCGA, IEU Open GWAS, and FinnGen for providing the public data. This study was supported by Hubei Provincial Department of Science and Technology, Innovation and Development Joint Fund (No. 2022CFD145). Young Talents Project of Hubei Provincial Administration of Traditional Chinese Medicine (No. ZY2023Q002).

Peer review information

Integrative Medicine Discovery thanks Zhen-Liang Fan and another anonymous reviewer for their contribution to the peer review of this paper.

Abbreviations

ccRCC, clear cell renal cell carcinoma; TCM, traditional Chinese medicine; TCGA, The Cancer Genome Atlas; GO, Gene Ontology; KEGG, Kyoto Encyclopedia of Genes and Genomes.

Citation

Li Y, Wang HY, Lv AQ, et al. Chinese medicine *Bupleuri Radix* inhibits the proliferation of renal clear cell carcinoma is related to RORγ. *Integr Med Discov*. 2025;9:e25005. doi: 10.53388/IMD202509005.

Executive editor: Xin-Yue Zhang.

Received: 03 December 2024; **Revised:** 01 January 2025; **Accepted:** 12 February 2025; **Available online:** 20 February 2025.

Background

Clear cell renal cell carcinoma (ccRCC) is a predominant urological malignancy, accounting for over 80% of all renal cell carcinoma cases and representing the most common histological subtype of malignant renal tumors [1, 2]. Although targeted therapies initially demonstrated potential in the treatment of ccRCC, their effectiveness is frequently compromised by the emergence of drug resistance and rapid tumor progression, resulting in suboptimal patient outcomes [3, 4]. This illustrates the demand for the creation of more effective targeted treatments.

Recent years have seen a growing interest in traditional Chinese medicine (TCM) among clinicians. TCM approaches often emphasize evidence-based treatments that substantially boost the quality of life for cancer sufferers. According to TCM principles, cancer is understood as a condition arising from "internal deficiency," with pathologies involving a blend of deficiency and excess. Specifically, ccRCC is characterized by a deficiency in "Qi" (vital energy), "Yin" (nourishing substance), and "Yang" (vital force), alongside dysfunctions in internal organs [5].

One notable TCM remedy is *Bupleuri Radix* (Chaihu), which is outlined in ancient literature such as the '*Yellow Emperor's Classic of Internal Medicine*'. *Bupleuri Radix* is known for its pungent, bitter, and slightly cold properties, and it is associated with the Shaoyang meridian. It is traditionally used to harmonize the exterior and interior, relieve liver depression, elevate yang, and alleviate fever [6]. Historically, *Bupleuri Radix* has been combined with other herbs to address conditions like bone metastases from renal cancer. For example, formulations such as Liu Wei Di Huang Wan combined with *Bupleuri Radix* have been used to tonify the kidneys and alleviate depressive symptoms in cancer patients [7].

Empirical evidence supports *Bupleuri Radix*'s therapeutic potential. Experiments have indicated that *Bupleuri Radix* is capable of hindering tumor growth in animal studies, reduce tumor size and weight, and alleviate associated depressive behaviors [8]. Additionally, extracts from *Bupleuri Radix* have been promising in hindering the differentiation of renal cancer cells in both in vitro and in vivo studies. *Bupleuri Radix* saponins, in particular, have been found to block renal cancer cells in the G0/G1 phase, induce apoptosis, and upregulate p53 protein expression [9].

In this research, we utilized various public databases to recognize the active ingredients and treatment targets of *Bupleuri Radix* in the context of ccRCC. We focused on Cedrenol, which emerged as the most bioavailable ingredient, and examined its high relevance to the gene *ROR*γ (*RORC*). Using a network pharmacology approach, a series of analyses were carried out by us to understand the function of *RORC* in ccRCC suppression. We have discovered that Cedrenol plays a crucial role as an active ingredient in *Bupleuri Radix*, and that *RORC* is a significant gene target through which *Bupleuri Radix* exerts its therapeutic effects on ccRCC. Knockdown of *RORC* was shown to inhibit tumor cell proliferation, thus validating its role as a target for ccRCC treatment.

Material and methods

Anticipating the active elements and targets of *Bupleuri Radix*

The Traditional Chinese Medicine Systematic Pharmacology Database was accessed at (http://tcmspw.com/tcmsp.php) to search for active ingredients of Bupleurum Chinense (*Bupleuri Radix*) using the keyword "chai hu/Radix Bupleuri". Screening criteria included oral bioavailability ≥ 30% and drug-likeness ≥ 0.18. Compounds not listed in the Traditional Chinese Medicine Systematic Pharmacology Database were further examined using the Swiss ADME platform (http://www.swissadme.ch/). Canonical SMILES of the identified compounds were accessed through the PubChem database (https://pubchem.ncbi.nlm.nih.gov/) and entered into the SwissTargetPrediction database can be accessed at (http://www.swisstargetprediction.ch/) to predict the chemical structures and gene targets.

Gene target identification for ccRCC

Data on gene expression for ccRCC were retrieved from The Cancer Genome Atlas (TCGA) with the keyword KIRC (https://portal.gdc.cancer.gov). Duplicates were removed, and RNAseq data from 33 tumor projects processed with STAR were downloaded. Data were collated in TPM format and integrated with RNAseq information sourced from UCSC XENA (https://xenabrowser.net/datapages/) and GTEx datasets, processed by Toil.Normal and tumor tissue data from TCGA and GTEx were extracted for comparative analysis.

Functional and pathway analysis

The intersecting gene targets from *Bupleuri Radix*, Cedrenol and ccRCC were analyzed for Gene Ontology (GO) and Kyoto Encyclopedia of Genes and Genomes (KEGG) pathway enrichment by uploading them to the DAVID database (https://david.ncifcrf.gov/). The target organism was set to Homo sapiens.

Data were visualized using microbiotics (https://www.bioinformatics.com.cn) and Sangerbox (http://sangerbox.com). Single-gene KEGG pathway and GO analyses for *RORC* were performed using the GSCALite database (https://guolab.wchscu.cn/GSCA).

Expression analysis and survival prediction

TIMER (http://timer.cistrome.org/) provided a visualization of *RORC* expression in a range of cancers [10], UALCAN (https://ualcan.path.uab.edu/), and UCSC XENA (https://xenabrowser.net/datapages/) to investigate the expression of *RORC* in normal and malignant tissues across different clinical subtypes, stages, and grades [11]. Using GSCALite, a Kaplan-Meier survival analysis was performed to evaluate the link between *RORC* expression and overall survival in ccRCC patients.

Examination of immune cell infiltration

Investigation into the connections between immune cells scores with *RORC* expression was performed [12]. Immune cell enrichment in ccRCC tissues was quantified using GSVA and visualized as chordal plots within the TIMER 2.0 data collection [13].

Evaluation of drug sensitivity and molecular docking

The analysis of drug sensitivity targeting *RORC* was performed with Spearman's correlation coefficients from GSCALite [14]. NCI-60 cell line RNA expression and drug activity data were sourced from the CellMiner database. Bubble and bar graphs were employed to visualize and analyze the correlations between *RORC* expression levels and drug sensitivity (IC_{50}) from the GDSC and CTRP databases.

Molecular docking was conducted using AutoDock Vina (http://vina.scripps.edu/) and AutoDock 1.5.6 software. Structures of small-molecule drugs and *RORC* were gathered from the PubChem and RCSB PDB databases (https://www.rcsb.org/). Binding affinities were calculated and visualized using PyMOL.

Scores reflecting gene effects

The analysis of gene effect scores was conducted using UALCAN, along with Broad's Achilles and Sanger's SCORE projects. Negative values in the normalized scores indicated cell growth inhibition or cell death following gene knockout, with gene effect scores inferred by Chronos [15].

Cell cultivation and RNA silencing techniques

The cell lines 786-O and OS-RC-2, which are human ccRCC, were obtained from Procell Life Science & Technology Co., Ltd. (Wuhan, China), in Procell's basal medium (RPMI-1640), cells were cultured with 1% penicillin/streptomycin and 10% fetal bovine serum, under conditions of 37 ˚C and 5% CO_2.

RORC-targeting siRNAs (si*RORC*-1, si*RORC*-2) Using the DharmaFECTTM 1 Transfection kit (Engreen Biosystem Co., Ltd.,

Beijing, China), the cells were transfected in accordance with the manufacturer's instructions. The siRNAs were sourced from Wuhan Biotech (Sangon Biotech, Wuhan, China).

Tests for cell growth and movement functions

Cell counting. Take 786-O and OS-RC-2 cells in logarithmic growth phase, digest the cells, count them, inoculate them uniformly in 6-well plates at a density of 5×10^4/well, 2 mL per well, and keep them in the incubator at 37 ˚C until the next day. On the next day, when the cells were in good growth condition, transfection or drug intervention, the condition of the cells was examined under the microscope on the third and fifth days of treatment. Remove the culture medium and take pictures under fluorescence microscope or light microscope for recording. Digest the cells with EDTA, centrifuge to remove the supernatant, add 1 mL of complete medium to dilute the cells, remove 10 μL of cytosol and place it on a coverslip to perform cell counting, and determine the proliferation rate of 786-O and OS-RC-2 cells through the Neubauer counting chamber technique. Each subgroup was repeated 3 times. The counting results were saved. According to the counting results, the cell growth trend was plotted.

EDU cell proliferation assay. Inoculate 786-O and OS-RC-2 cells into six-well plates at 10×10^4 per well, wait for the next day when the cell growth is stable, and intervene with plasmids or drugs for 48 h. After 48 h, replace the EDU reagent containing the corresponding concentration to be added to the 6-well plate and incubate for 6 h. Remove the medium containing EDU reagent and wash the cells with 1× PBS three times for 5 min each time. Afterward, the cells were exposed to 4% paraformaldehyde for half an hour. The samples were then permeabilized with 0.3% TritonX-100 (Biosharp, Anhui, China) immunostaining permeabilization solution for 15 min. Cells were washed three times with 1× PBS for 5 min each. The staining process was carried out with a reaction solution, and images were captured using fluorescence microscopy. The cytoplasm is green fluorescence and the nucleus is blue fluorescence.

Plate cloning. Inoculate: ccRCC cells at 500 per well in a 6-well plate and incubate for 1 week, observe the cells forming colonies under the microscope, and then perform plasmid transfection or drug-disturbed ccRCC cells and continue to incubate for 1 week, and change the complete culture medium every 2 d. Remove the complete medium and wash the cells rinsed with 1× PBS three times, 5 min per wash. Use 4% paraformaldehyde to fix the resulting colonies for 15 min, followed by three 5-min washes with 1× PBS. Slowly add 700 μL of crystal violet staining solution along the wall of each well for staining, shake the well plate to make the coverage uniform, and stain for 30 min. After recovering the crystal violet solution, rinse it with ultrapure water, and place it upside down in a fume hood to dry naturally. Take a picture with a printer and save the picture in tiff format.

Scratch experiment. Inoculate the healthy growing ccRCC cells into the 6-well plate at a density of 50×10^4 per well. After the cells were spread all over the well plates, the 786-O and OS-RC-2 cells were interfered with plasmids or drugs for 48 h. Scratch the cells mechanically using a 200 μL pipette tip and incubate them for 24 and 48 h, respectively. After culturing the cells for 24 h, the 6-well plate was taken out, and after aspirating the medium, the plate was carefully washed with PBS for 2 times and the medium was added and then placed under an inverted microscope again for observation and photographing, and then put into the 37 ˚C incubator for culture. After culturing the cells for 48 h, take out the 6-well plate, take out the culture medium, wash it twice with PBS and add the culture medium carefully, and then put it under the inverted microscope again for observation and photo recording.

Transwell experiment. Inoculate healthy 786-O and OS-RC-2 cells at a density of 30×10^4 per well into a 6-well plate. Following a 48-h treatment of 786-O and OS-RC-2 cells with plasmids or drugs, they were subjected to trypsin digestion, resulting in a cell suspension of 2×10^4 cells was added to 300 μL complete mediumin the upper chamber, a solution containing 2% fetal bovine serum was added, whereas the lower chamber was provided with a complete culture medium that included 10% fetal bovine serum. Following a 24-h incubation period, the medium was taken out from the well plates, and the cells were fixed using 4% glutaraldehyde for 15 min. The cells were carefully washed three times with PBS along the wall of the well plates to remove the fixative, and then 700 μL of crystal violet staining solution was slowly added to the lower chamber along the wall of each well for staining under light-avoidance conditions, and the well plates were shaken to make a uniform coverage and stained for 30 min. After recovering the crystal violet solution, rinse it with ultrapure water and place it upside down in a fume hood to dry naturally. Place under an inverted microscope for observation and photo recording.

Data analysis

Using GraphPad Prism 9.3.0 software, the experimental data were analyzed. Data were reported as mean plus or minus standard deviation. One-way ANOVA was used to determine statistical significance, with $P < 0.05$ as the criterion.

Results

Prediction of active ingredient target genes and disease gene acquisition in ccRCC for Chaihu

Table 1 lists the top 10 active ingredients of *Bupleuri Radix* with the highest oral bioavailability.

Among these, Cedrenol exhibited the highest oral utilization. To predict the chemical structure and gene targets of Cedrenol, we utilized the SwissTargetPrediction database.

Gene target analysis

A simple article overview chart (Figure 1). RNA sequencing data from 33 ccRCC tumor samples were obtained from the TCGA database and processed in Transcripts Per Million format. The intersection between Cedrenol's gene targets and those associated with ccRCC was analyzed. The results were visualized using Venn diagrams (Figure 2A, 2B), revealing a total of 108 common genes shared between Cedrenol and ccRCC.

Table1 Active ingredients of *Bupleuri Radix*

Mol ID	Molecule name	OB (%)	DL
MOL004658	Cedrenol	108.56	0.12
MOL000018	(+/−)-Isoborneol	86.98	0.05
MOL001789	Isoliquiritigenin	85.32	0.15
MOL004677	Ledol	82.78	0.12
MOL000244	()-Borneol	81.80	0.05
MOL000608	()-Terpinen-4-ol	81.41	0.03
MOL002338	136458-42-9	80.86	0.12
MOL004706	Spathulenol	80.01	0.12
MOL004644	Sainfuran	79.91	0.23

①Mol ID: ID of the active ingredient; ②Molecule Name: molecular name of the active ingredient; ③OB (%): bioavailability; ④DL: drug-like properties.

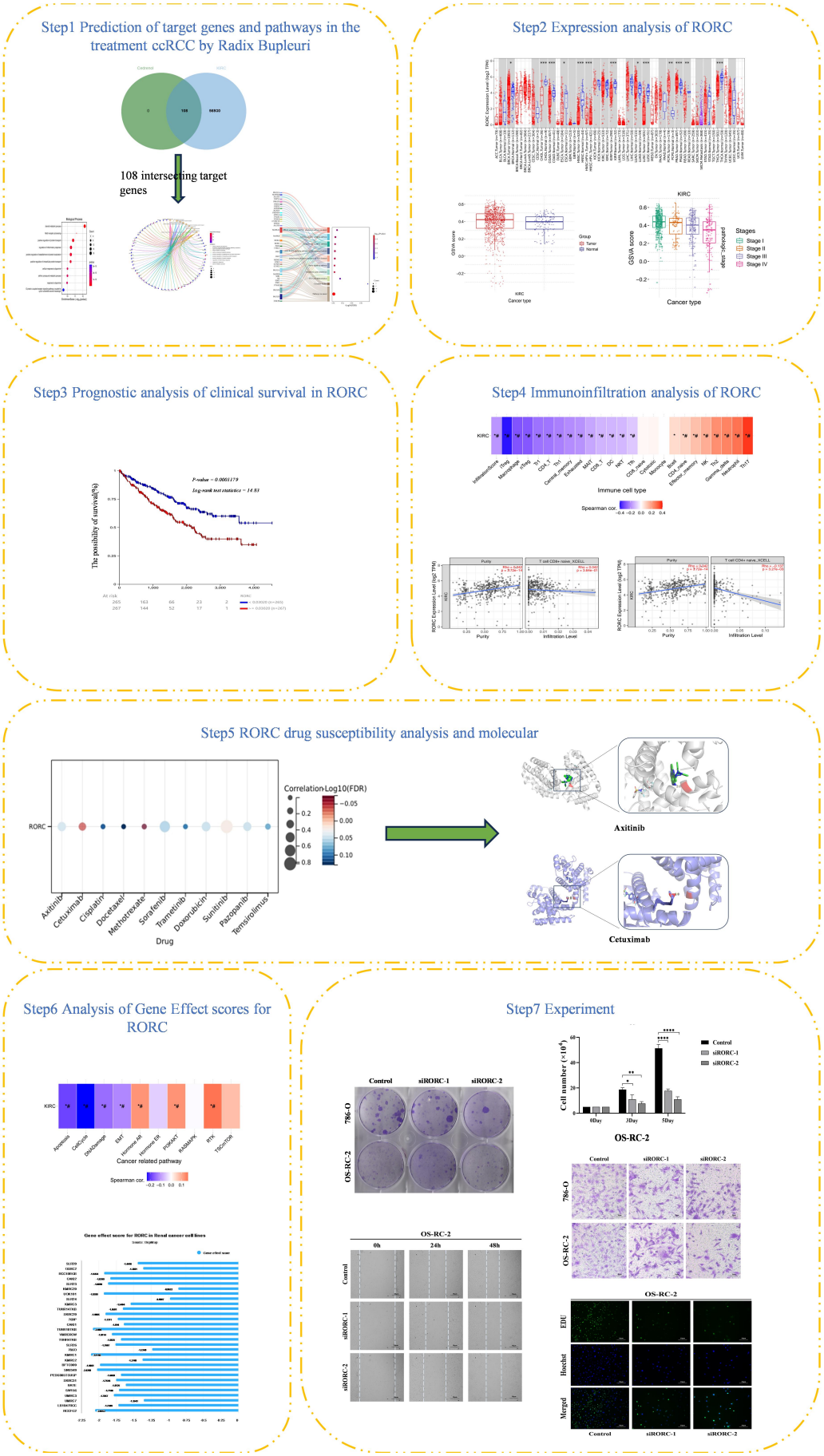

Figure 1 Overview of research design, to provide a more understandable research ideas. ccRCC, clear cell renal cell carcinoma.

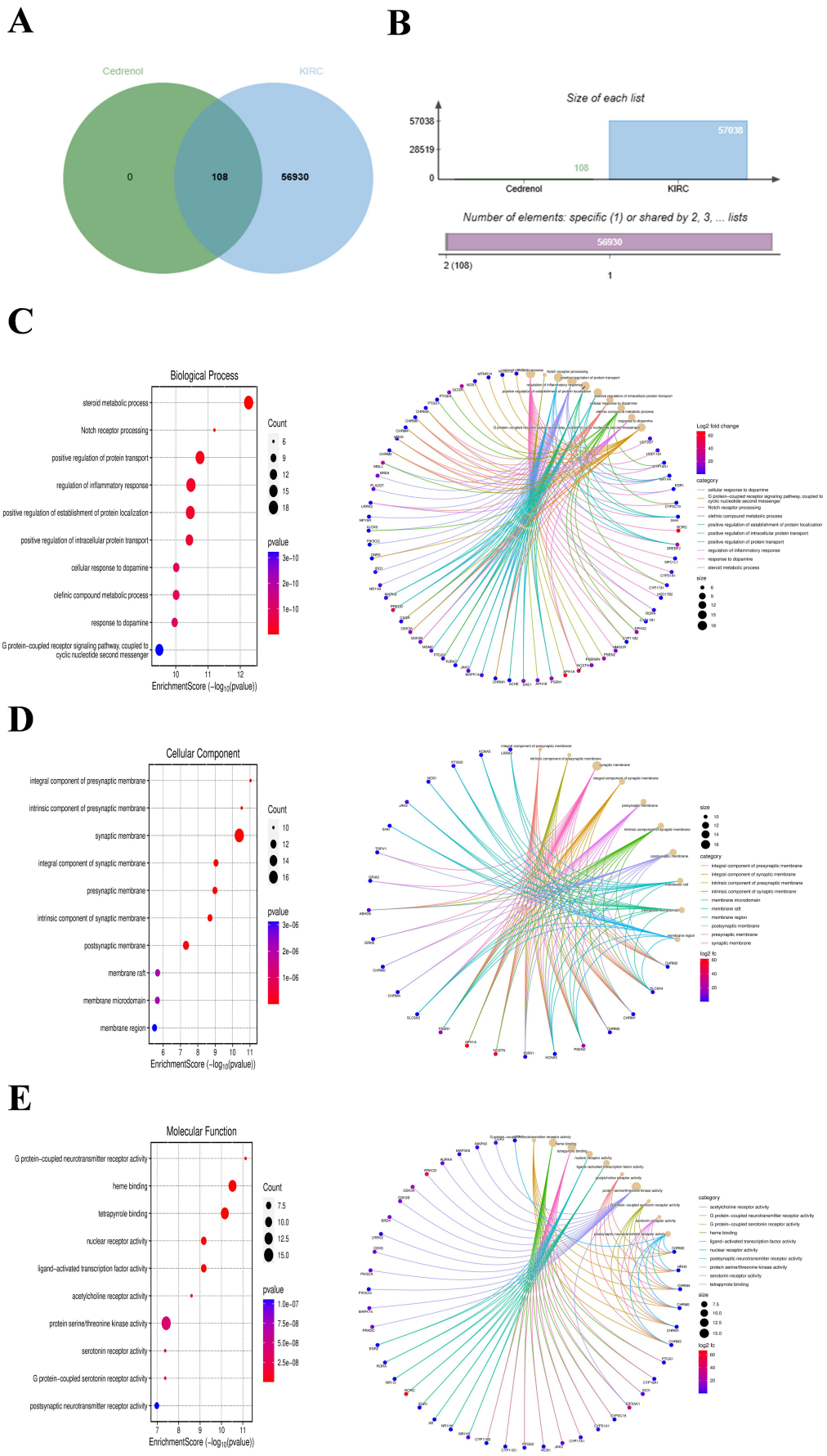

Figure 2 Prediction of target genes and pathways in the treatment ccRCC by *Bupleuri Radix*. (A, B) Venny's diagram of the active components of *Bupleuri Radix* and the ccRCC target gene. (C) Biological process analysis of intersecting genes. (D) Cellular component analysis of intersecting genes. (E) Molecular function analysis of intersecting genes.

Study of enrichment in GO and KEGG pathways

We analyzed the 108 genes shared by Cedrenol and ccRCC using GO functional analysis and KEGG pathway enrichment analysis. The gene expression data were organized and extracted in Transcripts Per Million format. Visualization of the GO and KEGG analyses was performed using the Microbiology Letters website.

Biological process. As depicted in Figure 2C, the identified genes are predominantly implicated in various biological processes, including the cellular response to dopamine, signaling pathways involving G protein-coupled receptors and cyclic nucleotide second messenger systems, Notch receptor processing, positive regulation of protein localization and transport, inflammatory response, and steroid metabolic processes. Notably, *RORC*, *APH1A*, and *PRKCD* exhibited the highest expression levels, with *RORC* demonstrating the most elevated expression index.

Cellular component. Figure 2D indicates that these genes are associated with integral components of the presynaptic membrane, membrane regions, and postsynaptic membranes.

Molecular function. According to Figure 2E, the genes are associated with G protein-coupled neurotransmitter receptor activity, serotonin receptor activity, heme binding, and nuclear receptor activity, and postsynaptic neurotransmitter receptor activity, with *RORC* emerging as the most plausible candidate. Further analysis using KEGG pathways indicated that the 108 genes are involved in pathways such as Th17 cell differentiation and circadian rhythm, as illustrated in Figure 3A, 3B. The Sankey and bubble maps illustrate that *RORC* is prominently involved in these pathways. Both GO and KEGG analyses underscore *RORC*'s significant role and its interaction with various pathways and gene products, warranting further investigation into its expression in ccRCC.

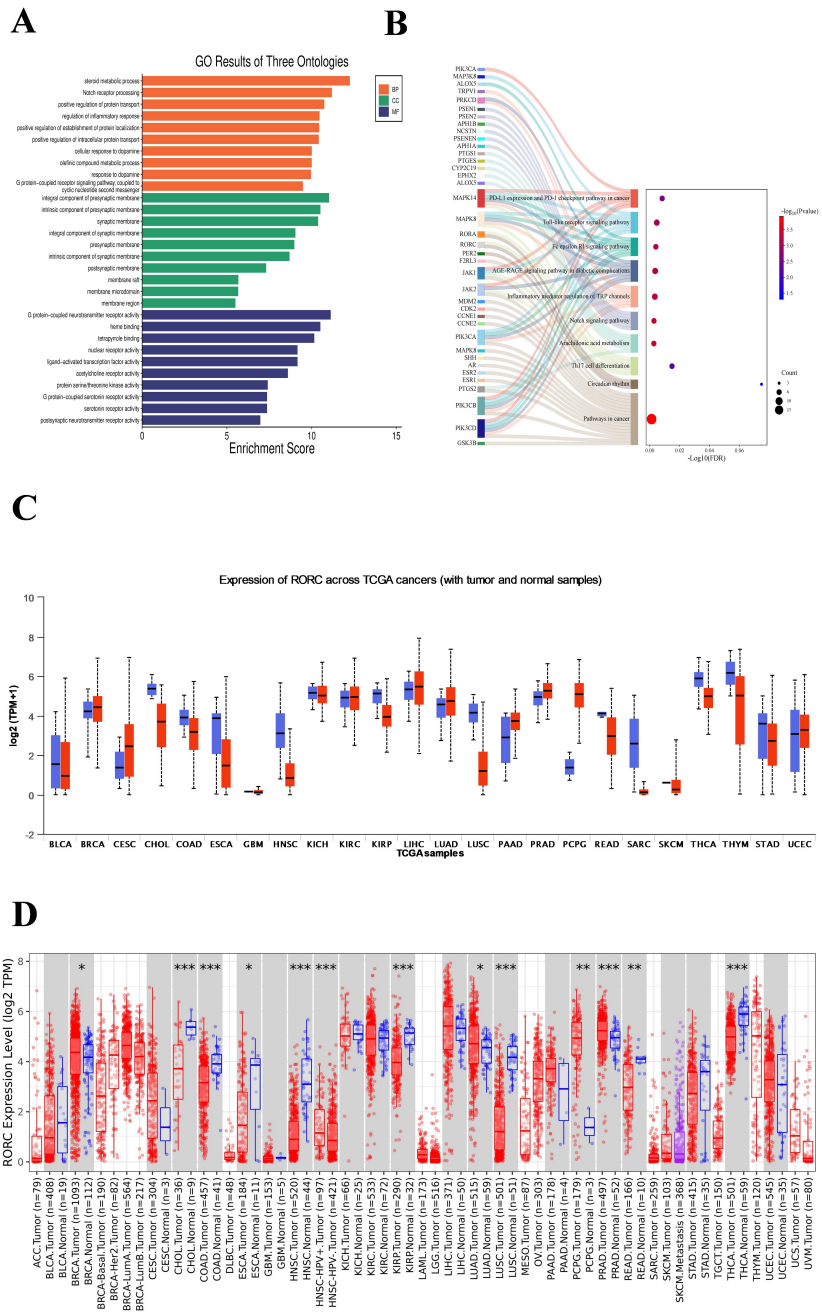

Figure 3 Pathway and expression analysis of *RORC*. (A) GO results of three ontologies. (B) Sankey Chart-Bubble Chart of *RORC*. (C) TIMER database visualizes differential *RORC* gene expression in pan-cancer. (D) UALCAN database visualizes differential expression of *RORC* genes in pan-cancer. $^{*}P < 0.5$; $^{**}P < 0.05$; $^{***}P < 0.005$. GO, Gene Ontology; BP, biological process; CC, cellular component; MF, molecular function.

RORC expression in renal clear cell carcinoma

To validate *RORC* expression in ccRCC, we analyzed its expression across different cancers using the TIMER and UALCAN databases (Figure 3C, 3D). Compared to normal tissues, *RORC* expression was markedly increased in breast cancer and kidney renal clear cell carcinoma. The UCSCXena and GSCALite databases were used for further analysis [16], showing increased *RORC* expression in ccRCC tumor tissues compared to normal tissues (Figure 4A). Among ccRCC subtypes, subtype 1 exhibited the highest *RORC* expression (Figure 4B). Stage-wise analysis revealed that *RORC* expression was highest in Stage 1 (Figure 4C, 4D, 4G). Additionally, higher expression of *RORC* was observed in women compared to men (Figure 4E), in ccA compared to ccB types [17] (Figure 4F), and in cancers without lymph node metastasis compared to those with metastasis (Figure 4H). Grade analysis also showed that *RORC* expression was higher in Grade 1 tumors compared to normal tissues (Figure 4I). According to Kaplan-Meier survival analysis, ccRCC patients with low *RORC* expression tend to have improved overall survival (Figure 4J).

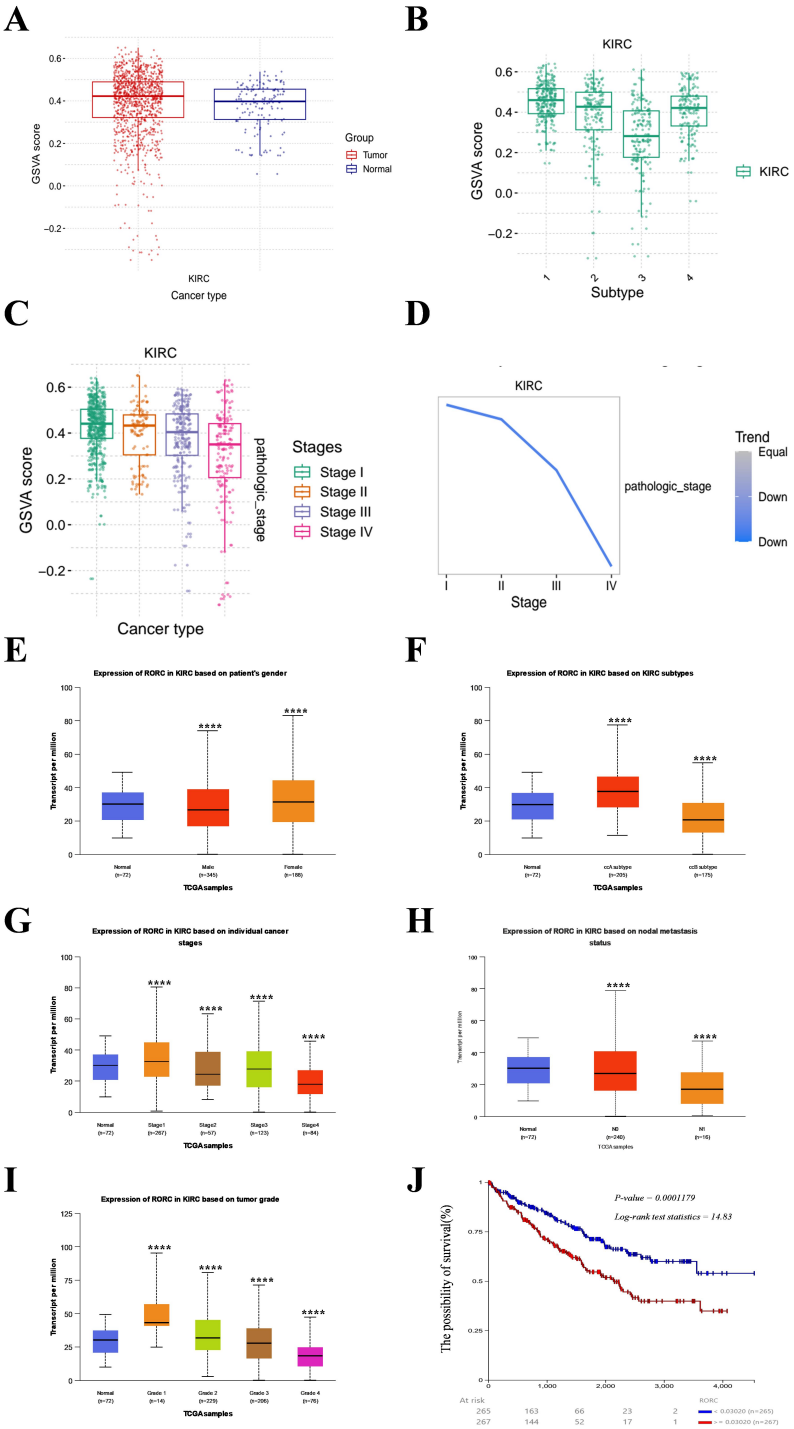

Figure 4 Analysis of *RORC* expression and clinical prognosis in ccRCC. (A) Expression of *RORC* in tumor tissues and paracancerous tissues in GSCALite database. (B) *RORC* expression in subtype typing. (C) *RORC* expression in stage typing. (D) A line graph showing the expression of *RORC* in stage typing. (E) UALCAN database shows *RORC* expression in women and men. (F) *RORC* expression in ccA and ccB typing. (G) Expression of *RORC* in Stage typing. (H) *RORC* and tumor lymph node metastasis. (I) UALCAN database analysis of *RORC* expression in Grade staging. (J) Clinical prognostic analysis of *RORC*. $^{****}P < 0.0005$.

Immune cell infiltration analysis

Our enrichment analysis suggested a relationship between *RORC* as well as immune cells infiltrating. The GSCALite database was used to assess immune cell infiltration scores in ccRCC (Figure 5A). The study results revealed connections with a variety of immune cells, including $CD4^+$ naïve, $CD8^+$ naïve, cytotoxic T cells, Tregs, Th17 cells, effector memory T cells, monocytes, macrophages, natural killer cells, neutrophils, gamma-delta T lymphocytes, and memory B cells. Visualization with the TIMER2.0 database (Figure 5B) revealed that *RORC* expression was negatively correlated with the infiltration of several immune cells, such as $CD4^+$ naïve T cells, $CD8^+$ naïve T cells, effector memory T cells, B cell memory, Tregs, NK cells, neutrophils, myeloid dendritic cells, macrophages, and monocytes, while positively correlating with gamma-delta T cells.

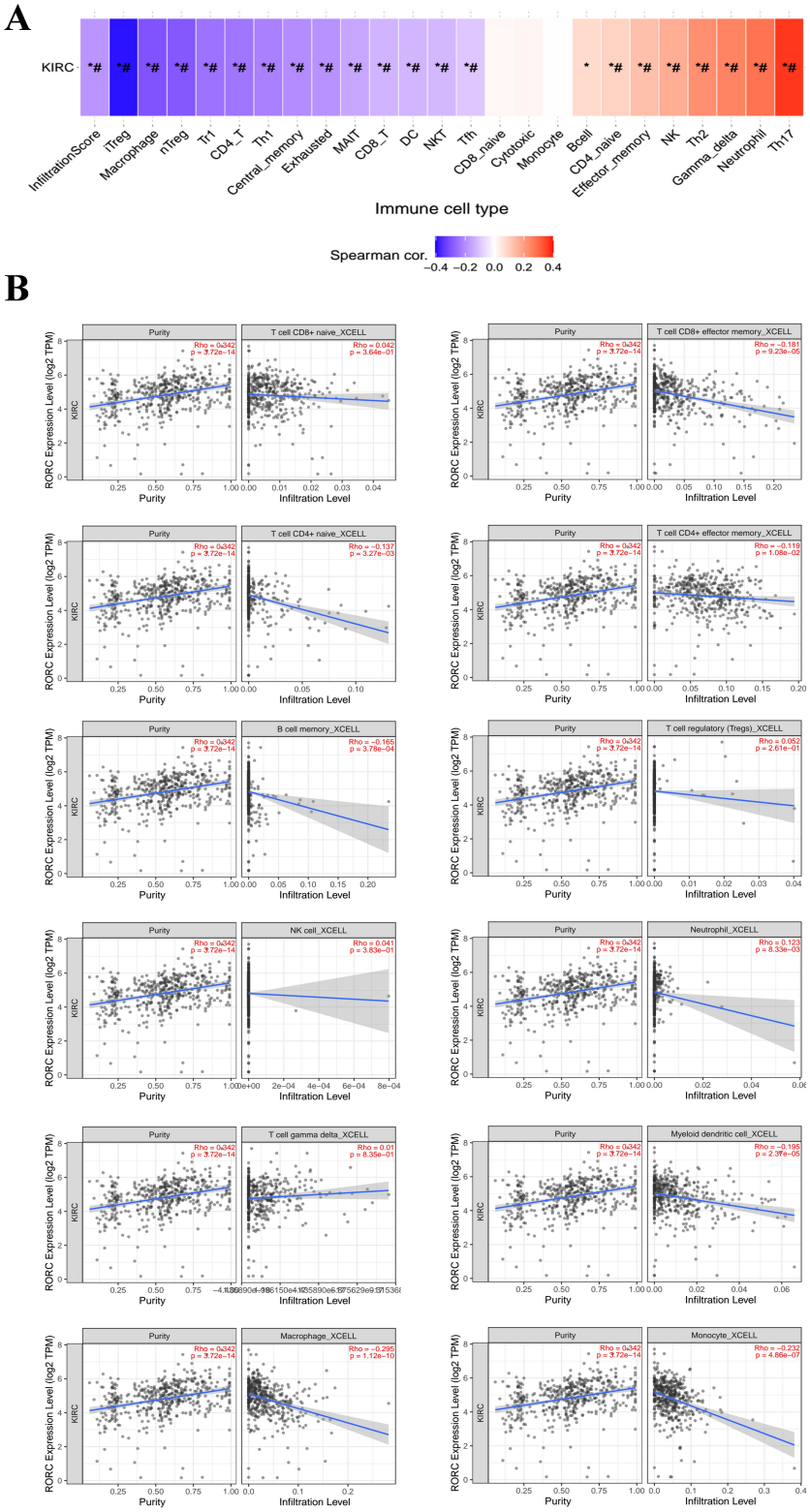

Figure 5 Immunoinfiltration analysis of *RORC*. (A) Enrichment analysis of *RORC* with immune cells. (B) Correlation analysis between *RORC* and immune cells. $^*P$ value $\leq$ 0.05; $^\#$FDR $\leq$ 0.05.

Correlation between *RORC* levels and drug response

The connection between *RORC* protein expression and drug effectiveness was evaluated using information from the GDSC and CTRP databases (Figure 6A). Increased *RORC* expression was associated with a higher sensitivity to several small molecule drugs utilized in renal cancer therapy. In particular, *RORC* expression was positively correlated with the IC_{50} value of Temsirolimus, there was an inverse relationship with the IC_{50} values of Cetuximab and Methotrexate (Figure 6B). Molecular docking simulations showed that *RORC* had high affinity for Axitinib (−11.82 kcal/mol), Docetaxel (−12.58 kcal/mol), Doxorubicin (−5.47 kcal/mol), Pazopanib (−8.84 kcal/mol), Sorafenib (−7.31 kcal/mol), Sunitinib (−7.54 kcal/mol), and Temsirolimus (−16.66 kcal/mol), while showing lower affinity for Cisplatin and Methotrexate (102.98 kcal/mol) (Figure 6C–6G).

Pathway enrichment and gene effect scores

Pathway enrichment analysis of *RORC* in ccRCC revealed that it is negatively correlated with pathways linked to apoptosis, regulation of the cell cycle, DNA damage, and process where epithelial cells transform into mesenchymal cells, while positively correlating with hormone AR signaling, PI3K/AKT, and RTK pathways (Figure 7A). Gene effect scores indicated that silencing *RORC* led to cell death in ccRCC cells, as evidenced by negative scores (Figure 7B).

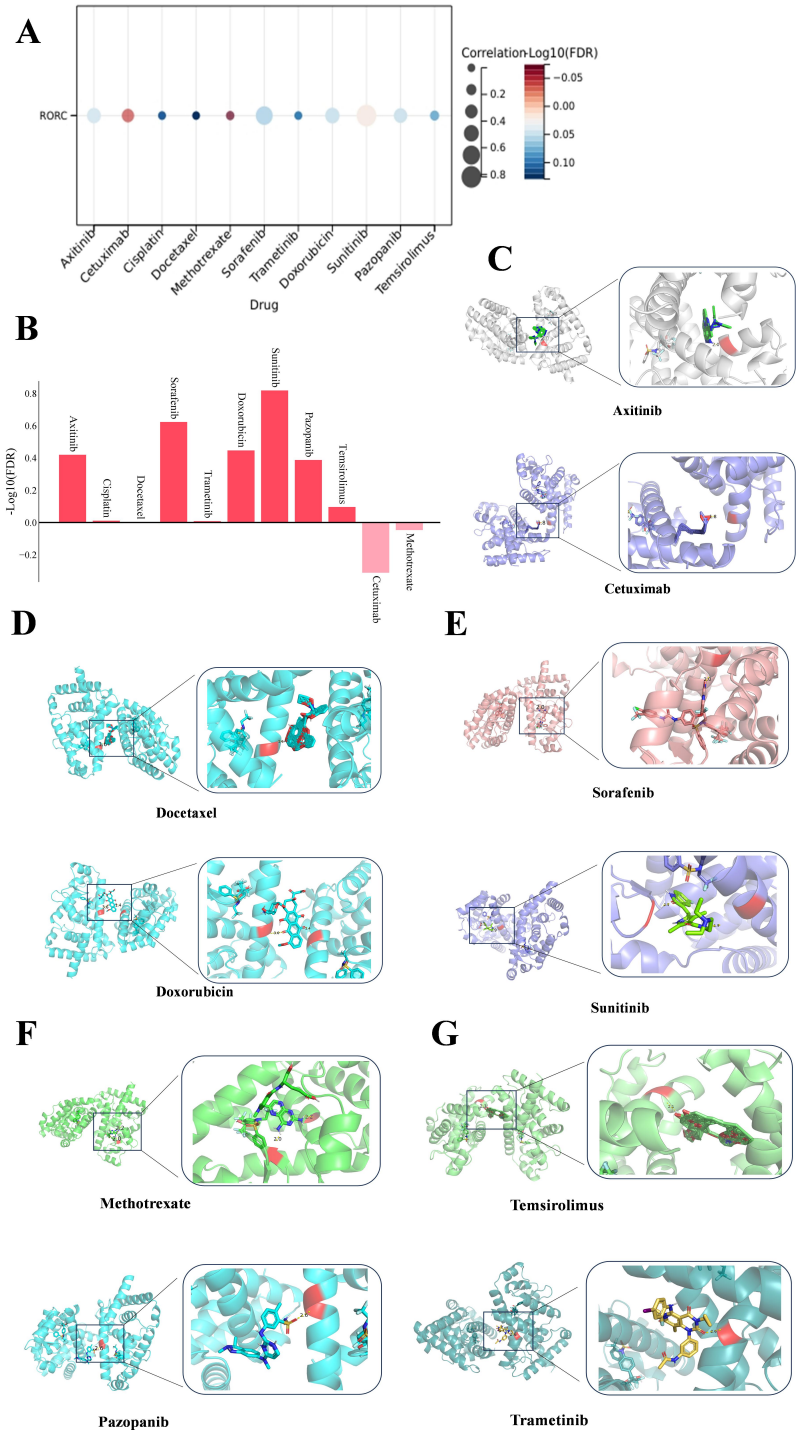

Figure 6 *RORC* drug susceptibility analysis and molecular. (A) Bubble chart demonstrating sensitivity analysis between *RORC* and drugs. (B) Bar graph showing correlation analysis between *RORC* and drugs. (C–G) *RORC* and molecular.

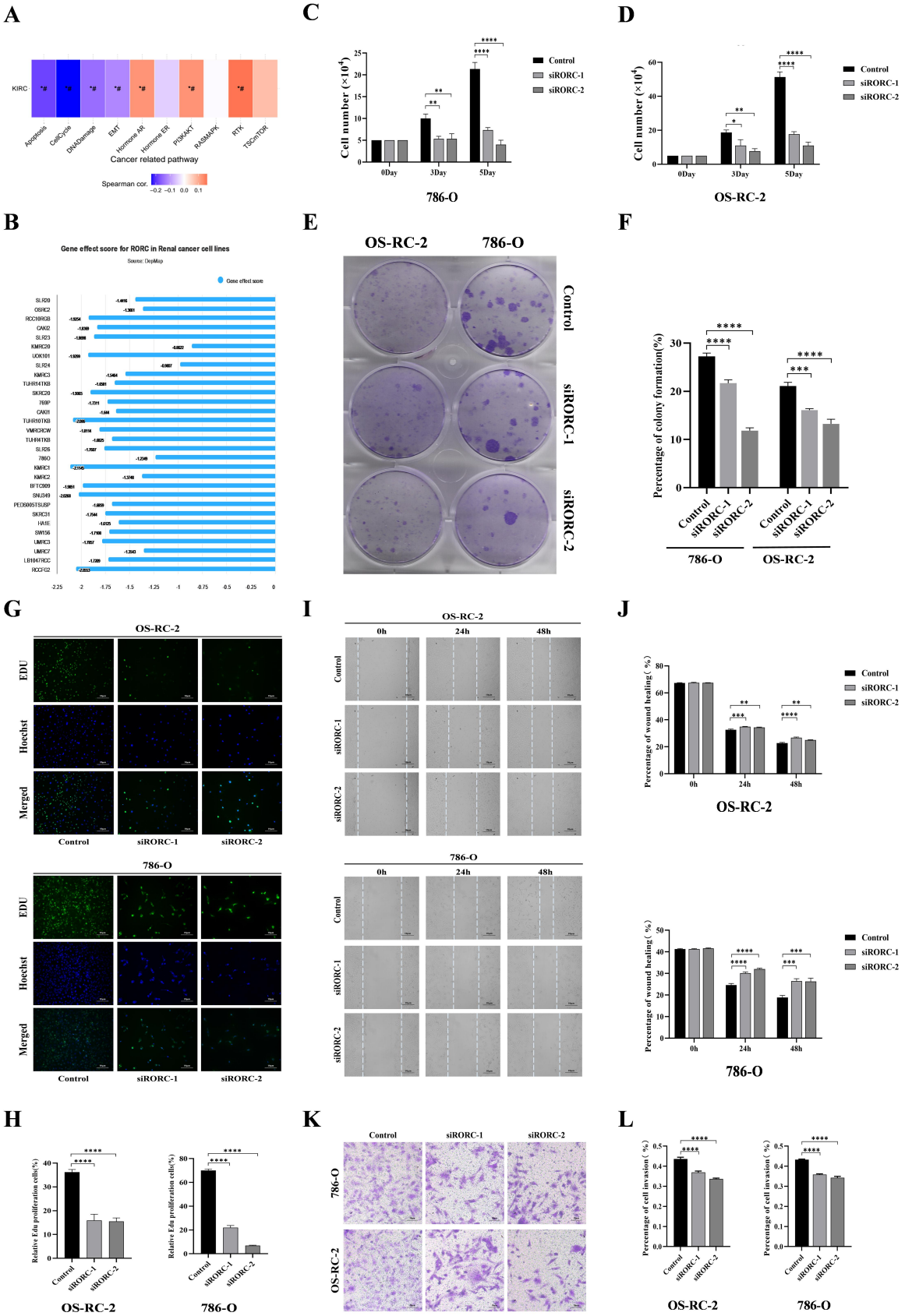

Figure 7 Experiment and analysis of gene effect scores for *RORC*. (A) *RORC* pathway enrichment analysis. $^{*}P$ value ≤ 0.05; $^{\#}$FDR ≤ 0.05. (B) Gene scores for *RORC*. (C, D) Changes in cell number after knockdown of *RORC*. (E, F) Ability of cells to form colonies after knockdown of *RORC*. (G, H) Cell proliferation ability detected by EDU assay after knockdown of *RORC*. Scale bar = 10 μm. (I, J) Detection of cell metastatic ability by scratch assay after knockdown of *RORC*. Scale bar = 10 μm. (K, L) Cell invasive ability detected by transwell assay after knockdown of *RORC*. Scale bar = 10 μm. $^{*}P < 0.5$; $^{**}P < 0.05$; $^{***}P < 0.005$; $^{****}P < 0.0005$.

In vitro cellular experiments

We knocked down the *RORC* gene in ccRCC cells in vitro, and then verified the inhibitory effect of *RORC* on ccRCC using assays to detect ability to proliferate and invade cells. In the results of cell counting (Figure 7C, 7D), plate cloning assay (Figure 7E, 7F), and EDU cell proliferation test (Figure 7G, 7H), we found that knockdown of *RORC* inhibited ccRCC cell proliferation. Then we tested the cell invasion ability with cell scratch assay (Figure 7I, 7J), transwell assay (Figure 7K, 7L), and found that the ability of ccRCC cells to invade was diminished following the silencing of the *RORC* gene, compared to the negative control group, suggesting that *RORC* plays a significant role as an oncogenic target in ccRCC.

Discussion

Recent advancements in oncology have increasingly integrated TCM, underscoring its potential to enhance patient outcomes through evidence-based methodologies. TCM posits that cancer arises from an "internal deficiency," characterized by an imbalance between "Yin", and "Yang", as well as a disturbance in the circulation of "Qi" and blood. This imbalance is thought to result in pathological accumulations and the development of cancer. The classical TCM text, *Huangdi Neijing*, advocates "warming the laborer" as a fundamental treatment strategy for deficiency diseases, while the *Compendium of Materia Medica* (written in 1552 to 1578 C.E.) identifies *Bupleuri Radix* as effective in addressing various symptoms, including malaria and fatigue. Contemporary research has demonstrated the efficacy of *Bupleuri Radix* in treating a range of cancers, including prostate, breast, cervical, and ccRCC [18–20]. This study specifically explores the therapeutic potential of *Bupleuri Radix* in ccRCC, employing network pharmacology to identify target gene loci and elucidate mechanisms, followed by in vitro validation.

Initially, we identified common target gene loci between *Bupleuri Radix*'s active ingredients and ccRCC. GO and KEGG pathway enrichment analyses highlighted genes such as *RORC*, *APH1A*, and *PRKCD*, with *RORC* emerging as a key player involved in pathways like Th17 cell differentiation and circadian rhythm. Given *RORC*'s prominence in these pathways, we further investigated its expression in ccRCC. Multiple database analyses revealed that *RORC* is upregulated in various malignancies, including ccRCC. Specifically, *RORC* expression was highest in subtype 1 and Stage 1 tumors, with notable differences between genders and between ccA and ccB staging. Furthermore, *RORC* levels were found to be elevated in tumors that did not have lymph node metastasis. According to the Kaplan-Meier survival analysis, it was demonstrated that reduced *RORC* expression is associated with improved overall survival, highlighting the importance of *RORC* as a possible biomarker and treatment target in ccRCC.

The progression and development of cancer are significantly influenced by immune cells, with immunotherapy emerging as a crucial strategy for advanced ccRCC [21, 22]. Our immune infiltration analysis demonstrated that *RORC* expression negatively correlates with the infiltration of several immune cell types, including $CD4^+$ T lymphocytes, macrophages, monocytes, B lymphocytes, natural killer cells, and $CD8^+$ T lymphocytes. This suggests that high *RORC* levels may suppress immune activity in ccRCC, highlighting *RORC* as a potential target for immunotherapeutic interventions.

Pharmacovigilance databases were used to investigate the link between *RORC* expression and drug sensitivity. There was an association between increased *RORC* expression and sensitivity to a number of small molecule drugs, including Axitinib, Cisplatin, Docetaxel, Sorafenib, Trametinib, Doxorubicin, Sunitinib, Pazopanib, and Temsirolimus. Molecular docking simulations indicated strong binding affinities for certain drugs, such as Axitinib and Docetaxel, suggesting that *RORC* could be targeted by these agents. This underscores the potential for integrating *RORC*-targeted therapies with existing treatment regimens for ccRCC. The development of targeted agents, including sorafenib, sunitinib, bevacizumab, pazopanib, and axitinib, has been made for RCC, which inhibit vascular endothelial growth factor and its receptor, together with everolimus and temsirolimus, which inhibit mechanistic target of rapamycin complex 1, being approved [23]. Several clinical trials have demonstrated that combining axitinib leads to longer overall survival and progression-free survival, along with a higher objective response rate, compared to sunitinib treatment [24, 25]. One research study concluded that pazopanib and sunitinib have equivalent effectiveness, yet pazopanib is advantageous in terms of safety and quality of life [26].

Further pathway enrichment and gene effect score analyses revealed that *RORC* is negatively correlated with apoptosis, cell cycle regulation, DNA damage, and EMT, while positively correlating with hormone AR signaling, PI3K/AKT, and RTK pathways. The gene effect scores suggested that inhibiting *RORC* caused cell death in ccRCC cells, supported by in vitro experiments demonstrating that *RORC* knockdown decreased cell proliferation, migration, and invasion.

In conclusion, our study provides compelling evidence that *RORC* plays a significant role in the progression of ccRCC. By inhibiting *RORC*, we observed reduced tumor cell proliferation and invasion, suggesting that *RORC* is a promising therapeutic target. The integration of TCM, such as *Bupleuri Radix*, with modern pharmacological approaches could enhance treatment strategies for ccRCC, potentially improving patient outcomes and advancing personalized medicine.

Conclusion

In this study, we leveraged a range of databases, analytical techniques, and in vitro experiments to provide comprehensive and multi-dimensional evidence on the part played by *ROR*γ (*RORC*) in ccRCC. Our analyses revealed that *ROR*γ is present in large amounts in ccRCC and plays a crucial regulatory role across several key aspects of cancer biology, including immune system modulation, drug sensitivity, and the processes of proliferation, migration and invasion.

Our findings demonstrate that *ROR*γ is a significant gene target of *Bupleuri Radix*, a TCM. By integrating bioinformatics analyses with experimental validation, we have shown that *ROR*γ not only serves as a potential biomarker for ccRCC but also as a therapeutic target. The elevated levels of *ROR*γ in ccRCC, coupled with its involvement in critical cancer-related pathways, underscores its importance in the pathology of the disease and its potential utility in enhancing therapeutic strategies.

Thus, our study supports the notion that targeting *ROR*γ could provide new opportunities for developing effective treatments for renal clear cell carcinoma, particularly in the context of integrating TCM approaches with modern therapeutic strategies.

Shortcomings

Firstly, we did not use the active ingredients of *Bupleuri Radix* and *Bupleuri Radix* for experiments when mining the active ingredients of *Bupleuri Radix* for cancer treatment gene targets through the TCM database, and only used the target gene *RORC* for relevant experimental validation. Secondly, in this study, we only analyzed by bioinformatics technology in the process of studying drug sensitivity and did not experimentally validate by clinical drugs. Thirdly, we verified the inhibitory effect of *RORC* knockdown on ccRCC during the experimental process, but this was only in the phenotypic study, and did not go deep into the specific pathway, which is a major drawback of our study.

References

1. Hou W, Ji Z. Generation of autochthonous mouse models of clear cell renal cell carcinoma: mouse models of renal cell carcinoma. *Exp Mol Med.* 2018;50(4):1–10. Available at: http://doi.org/10.1038/s12276-018-0059-4
2. Wang Q, Tang H, Luo X, et al. Immune-Associated Gene Signatures Serve as a Promising Biomarker of

Immunotherapeutic Prognosis for Renal Clear Cell Carcinoma. *Front Immunol.* 2022;13:890150. Available at: http://doi.org/10.3389/fimmu.2022.890150
3. Tang T, Du X, Zhang X, Niu W, Li C, Tan J. Computational identification and analysis of early diagnostic biomarkers for kidney cancer. *J Hum Genet.* 2019;64(10):1015–1022. Available at: http://doi.org/10.1038/s10038-019-0640-2
4. Infantino V, Dituri F, Convertini P, et al. Epigenetic upregulation and functional role of the mitochondrial aspartate/glutamate carrier isoform 1 in hepatocellular carcinoma. *Biochim Biophys Acta Mol Basis Dis.* 2019;1865(1):38–47. Available at: http://doi.org/10.1016/j.bbadis.2018.10.018
5. Chen RO, Jiang X, Zhang QL, Que CX, Zhang SH, Huang JC. Jin-Chang Huang's treatment of renal cancer metastasis based on the theories of "Shaoyang belongs to kidney" and "Shaoyang is the main bone". *J Chin Med.* 2023;38(4):766–770. (Chinese) Available at: http://doi.org/10.16368/j.issn.1674-8999.2023.04.127
6. Wang B, Zhang CH, Wang KQ. Wang Ke-Qiong's experience in the treatment of postoperative renal cell carcinoma with generalized eczema based on the method of reconciling Shaoyang. *New Tradit Chin Med.* 2021;53(14):121–124. (Chinese) Available at: http://doi.org/10.13457/j.cnki.jncm.2021.14.032
7. Li W, Zhou R, Zheng J, et al. Chaihu-Shugan-San ameliorates tumor growth in prostate cancer promoted by depression via modulating sphingolipid and glycerinphospholipid metabolism. *Front Pharmacol.* 2022;13:1011450. Available at: http://doi.org/10.3389/fphar.2022.1011450
8. Yan HC, Jiang W, Mao KR. Study on anti-tumor biomedical function of saikosaponin. *Mol Plant Breed.* 2022;20(2):689–696. (Chinese) Available at: http://doi.org/10.13271/j.mpb.020.000689
9. Vivian J, Rao AA, Nothaft FA, et al. Toil enables reproducible, open source, big biomedical data analyses. *Nat Biotechnol.* 2017;35(4):314–316. Available at: http://doi.org/10.1038/nbt.3772
10. Li T, Fu J, Zeng Z, et al. TIMER2.0 for analysis of tumor-infiltrating immune cells. *Nucleic Acids Res.* 2020;48(W1):W509–W514. Available at: http://doi.org/10.1093/nar/gkaa407
11. Luzzago S, Palumbo C, Rosiello G, et al. Effect of stage and grade migration on cancer specific mortality in renal cell carcinoma patients, according to clear cell vs. non-clear cell histology: A contemporary population-based analysis. *Urol Oncol.* 2020;38(5):506–514. Available at: http://doi.org/10.1016/j.urolonc.2020.02.004
12. Bindea G, Mlecnik B, Tosolini M, et al. Spatiotemporal dynamics of intratumoral immune cells reveal the immune landscape in human cancer. *Immunity.* 2013;39(4):782–795. Available at: http://doi.org/10.1016/j.immuni.2013.10.003
13. Uhlén M, Fagerberg L, Hallström BM, et al. Tissue-based map of the human proteome. *Science.* 2015;347(6220):1260419. Available at: http://doi.org/10.1126/science.1260419
14. Zhu Y, Hu Y, Wang P, et al. Comprehensive bioinformatics and experimental analysis of SH3PXD2B reveals its carcinogenic effect in gastric carcinoma. *Life Sci.* 2023;326:121792. Available at: http://doi.org/10.1016/j.lfs.2023.121792
15. Dempster JM, Boyle I, Vazquez F, et al. Chronos: a cell population dynamics model of CRISPR experiments that improves inference of gene fitness effects. *Genome Biol.* 2021;22(1):343. Available at: http://doi.org/10.1186/s13059-021-02540-7
16. Detterbeck FC, Stratton K, Giroux D, et al. The IASLC/ITMIG Thymic Epithelial Tumors Staging Project: proposal for an evidence-based stage classification system for the forthcoming (8th) edition of the TNM classification of malignant tumors. *J Thorac Oncol.* 2014;9(9 Suppl 2):S65–S72. Available at: http://doi.org/10.1097/JTO.0000000000000290
17. Purdue MP, Rhee J, Moore L, et al. Differences in risk factors for molecular subtypes of clear cell renal cell carcinoma. *Int J Cancer.* 2021;149(7):1448–1454. Available at: http://doi.org/10.1002/ijc.33701
18. Xiao K, Li K, Long S, Kong C, Zhu S. Potential Molecular Mechanisms of Chaihu-Shugan-San in Treatment of Breast Cancer Based on Network Pharmacology. *Evid Based Complement Alternat Med.* 2020;2020:3670309. Available at: http://doi.org/10.1155/2020/3670309
19. Xue JF, Ling Z, Jiao YN, Guan YL. The effect of Chaihu-shugan-san on cytotoxicity induction and PDGF gene expression in cervical cancer cell line HeLa in the presence of paclitaxel + cisplatin. *Cell Mol Biol (Noisy-le-grand).* 2021;67(3):143–147. Available at: http://doi.org/10.14715/cmb/2021.67.3.21
20. Wang B, Zhang CH, Wang KQ. Introduction of Ke-Qiong Wang's experience in treating postoperative renal cancer combined with generalized eczema based on conciliation and Shaoyang method. *New Chin Med.* 2021;53(14):121–124. (Chinese) Available at: http://doi.org/10.13457/j.cnki.jncm.2021.14.032
21. Gonzalez H, Hagerling C, Werb Z. Roles of the immune system in cancer: from tumor initiation to metastatic progression. *Genes Dev.* 2018;32(19–20):1267–1284. Available at: http://doi.org/10.1101/gad.314617.118
22. Meng L, Collier KA, Wang P, et al. Emerging Immunotherapy Approaches for Advanced Clear Cell Renal Cell Carcinoma. *Cells.* 2023;13(1):34. Available at: http://doi.org/10.3390/cells13010034
23. Hsieh JJ, Purdue MP, Signoretti S, et al. Renal cell carcinoma. *Nat Rev Dis Primers.* 2017;3:17009. Available at: http://doi.org/10.1038/nrdp.2017.9
24. Motzer RJ, Penkov K, Haanen J, et al. Avelumab plus Axitinib versus Sunitinib for Advanced Renal-Cell Carcinoma. *N Engl J Med.* 2019;380(12):1103–1115. Available at: http://doi.org/10.1056/NEJMoa1816047
25. Rini BI, Plimack ER, Stus V, et al. Pembrolizumab plus Axitinib versus Sunitinib for Advanced Renal-Cell Carcinoma. *N Engl J Med.* 2019;380(12):1116–1127. Available at: http://doi.org/10.1056/NEJMoa1816714
26. Motzer RJ, Hutson TE, Cella D, et al. Pazopanib versus Sunitinib in Metastatic Renal-Cell Carcinoma. *N Engl J Med.* 2013;369(8):722–731. Available at: http://doi.org/10.1056/NEJMoa1303989